Identification of differentially expressed genes induced by aberrant methylation in acute myeloid leukemia using integrated bioinformatics analyses

WEI-WEN CHEN, DA-BIN LIU, HONG-XIA XIAO, LI-JUN ZHOU and JIA QU

Medical Laboratories, Guangzhou Twelfth People's Hospital, Guangzhou, Guangdong 510620, P.R. China

Received April 13, 2022; Accepted August 11, 2022

DOI: 10.3892/ol.2022.13503

Abstract. Acute myeloid leukemia (AML) is a life-threatening hematological malignant disease. Methylation plays a crucial role in the etiology and pathogenesis of AML. The aim of the present study was to identify the aberrantly methylated differentially expressed genes (DEGs) in AML and determine the underlying mechanisms of tumorigenesis by conducting integrated bioinformatics analyses. Gene expression profiles (GSE109179, GSE142699, GSE49665 and GSE14772) and a gene methylation profile (GSE42042) were analyzed to identify the aberrantly methylated DEGs. Functional enrichment analyses of identified genes were conducted based on the Gene Ontology (GO) and Kyoto Encyclopedia of Genes and Genomes (KEGG) databases, and protein-protein interaction networks were established. Finally, the DEGs were validated by the reverse transcription-quantitative PCR analysis of patient samples. A total of seven downregulated hypermethylated genes and eight upregulated hypomethylated genes were validated. The differentially methylated DEGs were enriched in GO biological process terms associated with control of the immune response and the KEGG analysis indicated they were involved in AML, ferroptosis, TGF-β signaling and necroptosis pathways. Additionally, five downregulated hypermethylated genes that were also tumor suppressor genes (TSGs) were identified. *In vitro* assays revealed that the overexpression of transcription factor 7 (TCF7) and integrin a M (ITGAM) significantly inhibited the proliferation of HL60 cells; by contrast, the knockdown of TCF7 and CAMK4 promoted HL60 cell proliferation. Overall, the present study identified differentially methylated DEGs and pathways associated with AML, which may enhance the understanding of the underlying molecular mechanisms of AML. In the future, abnormally methylated oncogenes and TSGs may function as biomarkers and treatment targets for the diagnosis and treatment of AML.

Correspondence to: Dr Wei-Wen Chen, Medical Laboratories, Guangzhou Twelfth People's Hospital, 1 Tianqiang Road, Guangzhou, Guangdong 510620, P.R. China
E-mail: chenweiwen85144052@163.com

Abbreviations: AML, acute myeloid leukemia; BP, biological process; GO, gene ontology; DEG, differentially expressed gene; DMG, differentially methylated gene; PPI, protein-protein interaction

Key words: AML, bioinformatics, methylation, analysis, differentially expressed genes

Introduction

Acute myeloid leukemia (AML) is a life-threatening hematological cancer involving the myeloid cells generated by bone marrow (1). Furthermore, AML is a genetically heterogeneous clonal disorder, characterized by the accumulation of somatic modifications in hematopoietic progenitor cells that affect their normal self-renewal, proliferation and variation, all of which are involved in hematopoiesis (2). Hematopoietic stem cells also contribute to hematopoiesis via these processes (3). A clinical study demonstrated that allogeneic hematopoietic stem cell grafting was an effective therapeutic option for patients with secondary AML (4).

Microarray data obtained using high-throughput platforms are helpful for the identification of genes with significant changes in expression and epigenetic modifications during carcinogenesis, as well as for appraising the diagnostic and prognostic effectiveness of biomarkers (5). A previous study identified differentially methylated genes (DMGs) in cancers, including lung squamous cell carcinoma, oral squamous cell carcinoma, and head and neck squamous cell carcinoma (6). Nevertheless, such available studies on AML are limited, to the best of our knowledge.

Recently, it was reported that abnormal methylation of DNA can affect the incidence and development of cancer by influencing the chromatin structure, which modulates oncogenic or tumor suppressor genes (TSGs) at the transcriptional level (7,8). DNA methylation is an important epigenetic mechanism in cancer, which has been widely researched regarding its role in DNA injury repair, cell cycle control, apoptosis and angiogenesis, all of which are associated with the methylation of CpG islands (9) in the promoter regions of genes (10). Aberrant methylation can influence gene expression, particularly by reducing the expression of TSGs, leading to the occurrence and development of AML (11). Research has identified emerging groups of genes that are hypermethylated

and downregulated, or hypomethylated and upregulated in AML (12); however, the general profiles and pathways of the interacting proteins identified using microarrays remains poorly understood.

A limited number of studies have combined weighted correlation network analysis with competing endogenous RNA network construction (11) and used gene expression and methylation profile microarrays to research the development of AML (12,13). In the present study, four gene expression profiles, one gene methylation profile, an oncogene list and TSG list were comprehensively and scientifically evaluated using bioinformatics analysis. This included the identification of differentially expressed genes (DEGs) and DMGs using R software, and using Venn diagrams to identify the intersecting DEGs, DMGs, oncogenes and TSGs. Enrichment analyses were also conducted using the Gene Ontology (GO) and Kyoto Encyclopedia of Genes and Genomes (KEGG) databases (13). In addition, protein-protein interaction (PPI) networks (14) were constructed, and the microarray results for expression and methylation were validated in patient samples. The present study aimed to detect the aberrantly methylated DEGs between AML and control samples and identify the related GO terms (15) and KEGG pathways to determine the molecular mechanisms that underlie tumorigenesis in AML (16). Additionally, the study aimed to identify the abnormally methylated DEGs that were also oncogenes or TSGs, which may function as biomarkers and treatment targets for precise AML diagnosis and treatment in the future.

Materials and methods

Microarray data. The present study used four gene expression profile datasets (GSE109179, GSE142699, GSE49665 and GSE14772) and a gene methylation profile dataset (GSE42042) from the US National Center for Biotechnology Information (NCBI) Gene Expression Omnibus (GEO) database (http:, www.ncbi.nlm.nih.gov/geo/). The GSE109179 data were generated using the GPL15207 platform (Affymetrix PrimeView™ Human Gene Expression Array) and included whole blood samples from 9 patients with AML and 4 healthy controls (17). The GSE142699 data were generated using the GPL26945 platform [nanoString nCounter® Human microRNA (miRNA)] (18) and included whole blood samples from 24 patients with AML and 24 healthy donors. The GSE49665 data were generated using the GPL17547 platform (TU Graz miRNA array) and included whole blood samples from 52 patients with AML and 5 healthy donors (18). The GSE14772 data were generated using the GPL9081 platform (Agilent-016436 Human miRNA Microarray 1.0 G4472A; miRNA ID version) and included whole blood samples from 2 patients with AML and 7 normal controls (19). The GSE42042 data were derived from the GPL8490 platform [Illumina HumanMethylation27 BeadChip (HumanMethylation27 270596 v.1.2; Thermo Fisher Scientific)] and included 13 whole blood samples from patients with AML and 4 whole blood samples from healthy donors (20).

Identification of DEGs and DMGs. The abovementioned datasets were processed using R software (version 3.4.3; R Core Team). They were standardized using the wateRmelon (version 2.2.0; https://bioconductor.org/packages/wateRmelon/) and limma (version 3.52.2; https://bioconductor.org/biocLite.R) packages to identify DEGs and DMGs. The cut-off criteria for the DEGs and DMGs were $P<0.05$ and $|\log$ fold change (FC)$|>1.5$. The computer code used was as previously described (http:www.mdpi.com/1422-0067/19/6/1698/s1). The wANNOVAR tool (https://wannovar.wglab.org/) was used to convert the DMG identifiers into gene names. A list of oncogenes was obtained from the ON Gene database (http:ongene.bioinfo-minzhao.org/), and a list of TSGs was obtained from the TS Gene database (https:bioinfo.uth.edu/TSGene/index.html). An online Venn diagram tool (http:bioinfogp.cnb.csic.es/tools/venny/) was then employed to visualize the intersecting DEGs, DMGs, oncogenes and TSGs. Briefly, the upregulated hypomethylated oncogenes were identified as those in the overlap among hypomethylated genes, upregulated genes and oncogenes, while the downregulated hypermethylated TSGs were identified as those in the overlap among hypermethylated genes, downregulated genes and TSGs.

GO and KEGG enrichment analyses. The Database for Annotation, Visualization and Integrated Discovery (DAVID; http://david.abcc.ncifcrf.gov/) was used to perform GO and KEGG enrichment analyses. The lists of genes, comprising 45 upregulated hypomethylated genes and 60 downregulated hypermethylated genes were uploaded onto DAVID. $P<0.05$ was considered to indicate a statistically significant difference for both analyses. The biological process (BP) GO terms were ordered according to P-value, and the terms with the lowest P-values associated with the upregulated hypomethylated genes and downregulated hypermethylated genes were selected and visualized using bubble diagrams. The significantly enriched pathways in the KEGG analysis were visualized using the pathview package (https://pathview.uncc.edu/). The top 10 KEGG pathways associated with the upregulated hypomethylated genes and downregulated hypermethylated genes were selected and visualized using bubble diagrams. FunRich 3.0 software (https://www.funrich.org/) was used to visualize the pathways associated with the genes of interest (21).

PPI network construction and module analysis. Construction of PPI networks enables the clarification and visualization of potential molecular mechanisms that are pivotal in oncogenesis. The STRING database (https: string-db.org/) and FunRich software were used to construct PPI networks. In addition, functional enrichment analysis of the five downregulated hypermethylated TSGs was performed using FunRich software, and the top five pathways in each analysis were selected. Notably, no upregulated hypomethylated oncogenes were identified.

Validation of selected genes. To confirm the integrated bioinformatics analyses-based findings, 15 DEGs (Table I), i.e., 10 downregulated hypermethylated genes [transcription factor 7 (TCF7), charged multivesicular body protein 7 (CHMP7), phosphatidylinositol-4,5-bisphosphonate 3-kinase catalytic subunit α (PIK3CA), solute carrier family 39 member 8 (SLC39A8), cytochrome B-245 β chain (CYBB), inhibitor of DNA binding 3, HLH protein (ID3), calcium/calmodulin

Table I. List of the 15 differentially expressed genes.

Gene	log_2FC	P-value	q-value
TCF7	-1.200	0.003	0.239
CHMP7	-1.233	0.004	0.170
PIK3CA	-0.784	0.011	0.361
SLC39A8	-0.611	0.002	0.225
CYBB	-0.677	0.016	0.399
ID3	-1.238	0.003	0.254
CAMK4	-1.266	0.026	0.462
VCL	0.617	0.031	0.487
ZBP1	0.877	0.005	0.274
TFDP1	0.867	0.005	0.279
ITGAM	2.487	0.002	0.232
ADRB2	0.885	0.012	0.365
SUFU	-0.672	0.002	0.219
PLEKHO1	-1.045	0.013	0.376
BNIP3L	-0.761	0.019	0.420

TCF7, transcription factor 7; CHMP7, charged multivesicular body protein 7; PIK3CA, phosphatidylinositol-4,5-bisphosphonate 3-kinase catalytic subunit α; SCL39A8, solute carrier family 39 member 8; CYBB, cytochrome B-245 β chain; ID3, inhibitor of DNA binding 3, HLH protein; CAMK4, calcium/calmodulin dependent protein kinase IV; VCL, vinculin; ZBP1, Z-DNA binding protein 1, transcription factor Dp-ZBP1; TFDP1, transcription factor Dp-1; ITGAM, integrin α M; ADRB2, adrenoceptor β 2; SUFU, SUFU negative regulator of Hedgehog signaling; PLEKHO1, pleckstrin homology domain containing O1; BNIP3L, BCL2 interacting protein 3 like.

dependent protein kinase IV (CAMK4), SUFU negative regulator of Hedgehog signaling (SUFU), pleckstrin homology domain containing O1 (PLEKHO1) and BCL2 interacting protein 3 like (BNIP3L)] and five upregulated hypomethylated genes [vinculin (VCL), Z-DNA binding protein 1 (ZBP1), transcription factor Dp-1 (TFDP1), integrin α M (ITGAM) and adrenoceptor β 2 (ADRB2)] were randomly selected for validation using reverse transcription-quantitative polymerase chain reaction (RT-qPCR). Additionally, next-generation sequencing-based bisulfite sequencing/PCR was used to validate the methylation status in the promoters of six of the aforementioned genes (CAMK4, ITGAM, CYBB, SLC39A8, SUFU and VCL). Targeted bisulfite sequencing (TBS) was applied to analyze the methylation status. Validation of the selected genes was fulfilled using blood samples from five patients with AML, and five healthy controls. The samples were collected by Guangzhou Twelfth People's Hospital (Guangzhou, China) between January 2019 and December 2020. Information on the patients with AML is presented in Table II. Inclusion criteria for selecting the patients with AML were as follows: Histologically confirmed AML with >20% blasts; AML refractory to or relapsed after initial treatment, with no more than three prior lines of therapy; age ≥18 years; and Eastern Cooperative Oncology Group performance status ≤2. The exclusion criteria were: Treatment-related AML or acute promyelocytic leukemia; active malignancies within

Table II. Clinical data of patients with acute myeloid leukemia (n=5).

Characteristic	Cases (n)
Age <60 years	5
Sex	
Female	3
Male	2
Neoadjuvant treatment	
Yes	3
No	2
Survival status	
Alive	5
Dead	0

12 months, excluding those with a negligible risk of metastasis or death; clinical evidence of active central nervous system leukemia at the time of screening. Independent t-tests were used to calculate P-values to determine if the differences between the AML and control groups were significant for the 15 DEGs. Genes with P<0.05 and the absolute value of FC >2.0 were considered as DEGs.

RT-qPCR. Total RNA was extracted from 300 μl blood using TRIzol® reagent (Invitrogen; Thermo Fisher Scientific, Inc.) according to the manufacturer's protocol, and placing at 4˚C for 5 min, then adding 0.24 ml chloroform, shaking violently for 15 sec and standing at 4˚C for 3 min. The mixture was then centrifuged at 4,000 x g at 4˚C for 15 min, and the upper aqueous phase was transferred to a new tube. An equal volume of isopropyl alcohol was added, mixed in and left to stand at -20˚C for 20 min. The supernatant was removed by centrifugation at 4,000 x g for 15 min at 4˚C, and the precipitate was washed with 1 ml 75% DEPC alcohol, centrifuged at 8,000 rpm for 5 min at 4˚C and the liquid discarded. After drying at room temperature, 30 μl DEPC-treated ddH_2O was added to the residue to dissolve the RNA. After determining the concentration of 1.5 μl sample solution using an ultra-micro ultraviolet analyzer, the RNA was frozen at -80˚C for future use. Using 2 μg total RNA as template in a total system volume of 10 μl, RT-qPCR was performed using a Bestar™ qPCR RT Kit (DBI Bioscience) according to the manufacturer's instructions. The following thermocycling conditions were used for qPCR amplification: 95˚C for 2 min, 94˚C for 20 sec, 58˚C for 20 sec and 72˚C for 20 sec, for 40 cycles. Melting curve analysis was performed at 94˚C for 30 sec, 65˚C for 30 sec and 94˚C for 30 sec. The primer sequences used are listed in Table III. GAPDH was used as the reference gene. The analysis of each sample was repeated three times using the $2^{-\Delta\Delta Cq}$ method (22).

TBS-PCR. The *TBS-PCR* amplification primer pool (including upstream primer pool A and downstream primer pool B, with primer lengths between 26 and 36 bases, annealing temperatures of 55-65˚C and amplicon length 150-250 bp) was designed using Acegen Targeted Methyl Panel, (a multi-targeted PCR primer designing software system for bisulfite sequencing;

Table III. Sequences of the primer pairs for analysis of differentially expressed genes by reverse transcription-quantitative PCR.

Gene	Forward (5'-3')	Reverse (5'-3')
GAPDH	TGTTCGTCATGGGTGTGAAC	ATGGCATGGACTGTGGTCAT
TCF7	TTGATGCTAGGTTCTGGTGTACC	CCTTGGACTCTGCTTGTGTC
CHMP7	AAGCCTCTCAAGTGGACTCTT	ACAGACGATACACCTCCTCAG
PIK3CA	AGTAGGCAACCGTGAAGAAAAG	GAGGTGAATTGAGGTCCCTAAGA
SLC39A8	ATGCTACCCAAATAACCAGCTC	ACAGGAATCCATATCCCCAAACT
CYBB	ACCGGGTTTATGATATTCCACCT	GATTTCGACAGACTGGCAAGA
ID3	AAATCCTACAGCGCGTCATC	AAAGCTCCTTTTGTCGTTGGA
CAMK4	AGTTCTTCTTCGCCTCTCACA	CATCTCGCTCACTGTAATATCCC
VCL	CTCGTCCGGGTTGGAAAAGAG	AGTAAGGGTCTGACTGAAGCAT
ZBP1	GAAGAGCAAAGTCAGCCTCA	TGATGTTCCCGTGTCCAATC
TFDP1	AATTGAAGCCAACGGAGAACTC	CGGTCTCTGAGGCGTACCA
ITGAM	ACTTGCAGTGAGAACACGTATG	TCATCCGCCGAAAGTCATGTG
ADRB2	GCCTGTGCTGATCTGGTCAT	AATGGAAGTCCAAAACTCGCA
SUFU	GCCTGAGTGATCTCTATGGTGA	TCTCTCTTCAGACGAAAGGTCAA
PLEKHO1	GGGACCAGCTCTACATCTCTG	TGGAGTGGGCAAGAGTAAACT
BNIP3L	ATGTCGTCCCACCTAGTCGAG	TGAGGATGGTACGTGTTCCAG

TCF7, transcription factor 7; CHMP7, charged multivesicular body protein 7; PIK3CA, phosphatidylinositol-4,5-bisphosphonate 3-kinase catalytic subunit α; SCL39A8, solute carrier family 39 member 8; CYBB, cytochrome B-245 β chain; ID3, inhibitor of DNA binding 3, HLH protein; CAMK4, calcium/calmodulin dependent protein kinase IV; VCL, vinculin; ZBP1, Z-DNA binding protein 1, transcription factor Dp-ZBP1; TFDP1, transcription factor Dp-1; ITGAM, integrin α M; ADRB2, adrenoceptor β 2; SUFU, SUFU negative regulator of Hedgehog signaling; PLEKHO1, pleckstrin homology domain containing O1; BNIP3L, BCL2 interacting protein 3 like.

http://symech.fgg.uni-lj.si/). The sequences of the primer pairs are listed in Table IV. Firstly, 1 μg genomic DNA was converted using an ZYMO EZ DNA Methylation-Gold Kit (Zymo Research Corp.) and 5% of the elution products were used as templates for 35 cycles of PCR amplification with a KAPA HiFi Hot Start Uracil+ Ready Mix PCR Kit (Kapa Biosystems; Roche Diagnostics). The following thermocycling conditions were used for qPCR amplification: 98˚C for 2 min, followed by 98˚C for 15 sec, 63˚C for 2 min and 72˚C for 30 sec, then 72˚C for 1 min and hold at 4˚C. The amplification products were purified using 1X magnetic beads (Agencourt AMPure XP; Beckman Coulter) to remove contaminants, and the recovered products were used for DNA library preparation. The specific target band was detected for the success of library construction through electrophoresis. For each sample, the bisulfite PCR amplification products of multiple genes were pooled equally and then 5'-phosphorylated, 3'-dA-tailed and ligated to a barcoded adapter (VAHTS DNA Adapters set3-set6 for Illumina N808; Vazyme Biotech, Co., Ltd.) using T4 DNA ligase (cat no. M0202L; New England Biolabs, Inc.). The prepared library (34.5 ng/μl; 30 μl) was quantified using a Qubit™ 3.0 fluorometer (Thermo Fisher Scientific, Inc.) and Agilent 2100 Bioanalyzer (Agilent Technologies, Inc.). The sequencing strategy (NovaSeq Reagent Kit; PE150; Illumina Inc.) was paired-ended (PE) index sequencing with a sequencing reads length of PE150 performed using an Illumina platform (Novaseq 6000; Agilent Technologies, Inc.). Differentially methylated regions were identified based on comparison of the methylation levels of cytosines between samples from the two groups using the Mann-Whitney U-test. A mean methylation difference >0.05 and P<0.05 were considered statistically significant. The statistical analyses were performed using R.

Survival analysis. SPSS software (IBM Corp.) was used to perform a survival analysis to determine the association between patient survival rates and DEGs. The data on 140 patients with AML were acquired from The Cancer Genome Atlas (TCGA). The patients were divided into high and low expression groups according to the median value of each gene. Kaplan-Meier survival curves were drawn. Additionally, Cox regression analysis (23) was used to calculate hazard ratio (HR) values for the Kaplan-Meier plots and the log-rank test was used to calculate P-values.

Cell culture and transfection. HL60 AML cells (Shanghai EK-Bioscience) were sustained in minimum elementary RPMI-1640 (C11875500BT; Gibco; Thermo Fisher Scientific, Inc.) containing 10% fetal bovine serum (cat. no. 04-001-1A; Biological Industries) and 1% penicillin and streptomycin (15140-122; Gibco; Thermo Fisher Scientific, Inc.). The HL60 cells was maintained in a humidity incubator with 5% CO_2 at 37˚C. LV003-TCF7, LV003-ITGAM, LV003-CAMK4, LV003, small interfering (si)-homo-TCF7, si-homo-ITGAM, si-homo-CAMK4 and negative control (siRNA-NC) sequences were transfected into the HL60 cells using EndoFectin™-Max (EF004; GeneCopoeia, Inc.) according to the manufacturer's protocol. The overexpression vectors were designed by Anhui GENERAL BIOL and the interference fragments were designed by Suzhou GenePharma, Co., Ltd. The overexpression vectors were based on an LV003 lentiviral vector plasmid backbone (Forevergen Bioscoences Co., Ltd.). The sequences

Table IV. Sequences of the primer pairs used for analysis of differentially expressed genes using targeted bisulfite sequencing.

Amplicon	Left primer	Right primer
CAMK4-1	GGTTAGTTGGTGTTA	CTTTCTCTCTCCC
	GGTGGGAGGGA	AAACTATAACTACC
CAMK4-2	GGATTATTGGATYGA	CCTAAATAAAAAT
	YGGTTTTAATAGGGATG	TAACTCTCTCTCAAAACACT
CYBB	GTTTTAGTTTTTTTTGAGT	CCAATAATAAACCACAT
	AGTTGGGATTATAGGTGT	ATATAACAATAATCCCAT
ITGAM	GGAAATATTTGAGAGTT	CCAATAATAAACCA
	GTATAGGAAGGAA	AATTATACAAAAAC
SLC39A8-1	GGGGTTATTTTGGTTT	TCCCCCTTTATCCTCTT
	GGGTTTTTTTTTGAGGGT	TATCTCAAACTCTCCA
SLC39A8-2	GTTTTTTATAAATAAG	CTCCATTTCAACAAATT
	GGGAGGAGGGTTTTG	AATTTCATCAAAATCAC
SUFU-1	GAGTTTYGGAAGTTAATTT	CCAAACCAATCCT
	TTATAGTTTTGGAGTA	TAAACCCTTAACTCT
SUFU-2	GGATTATGTGATAAG	CCCCAAAAAAAAAAATT
	GGGAGGAAGGA	CCTCTACCATAAAATCCT
VCL-1	GTGTGAAGGGAAAAG	CCCCTCCCCCATT
	TTGAGGAGGGGA	CCTAAAAAAAAAACCT
VCL-2	GAGTATTTYGAAAAG	CATTATCACCAAATAAA
	GGATTAGTAGGAGTGG	AAATCTACTATACCACC

CAMK4, calcium/calmodulin dependent protein kinase IV; CYBB, cytochrome B-245 β chain; ITGAM, integrin α M; SCL39A8, solute carrier family 39 member 8; SUFU, SUFU negative regulator of Hedgehog signaling; VCL, vinculin.

Table V. siRNA sequences.

	Sequence	
siRNA	Sense (5'-3')	Antisense (5'-3')
si-homo-ITGAM-479	GCATCATCCCACATGACTT	AAGTCATGTGGGATGATGC
si-homo-ITGAM-1123	GCTGGTGGAGTCTTTCTAT	ATAGAAAGACTCCACCAGC
si-homo-ITGAM-2931	GCTGAACCAGACTGTCATA	TATGACAGTCTGGTTCAGC
si-TCF7-homo-152	TCAAGTCGTCGCTCGTGAA	TTCACGAGCGACGACTTGA
si-TCF7-homo-276	GAGACTCTTCCCGGACAAA	TTTGTCCGGGAAGAGTCTC
si-TCF7-homo-671	GCGGATATAGACAGCACTT	AAGTGCTGTCTATATCCGC
si-CAMK4-homo-1204	AGUUAAAGGUGCAGAUAUAAA	UUUAUAUCUGCACCUUUAACU
si-CAMK4-homo-365	GGAGGAGAACUGUUUGAUAGG	CCUAUCAAACAGUUCUCCUCC
si-CAMK4-homo-172	CAUUGUGUACAGAUGCAAACA	UGUUUGCAUCUGUACACAAUG
si-NC	UUCUCCGAACGUGUCACGUTT	ACGUGACACGUUCGGAGAATT

ITGAM, integrin α M; TCF7, transcription factor 7; CAMK4, calcium/calmodulin dependent protein kinase IV; si, small interfering; NC, negative control.

of the siRNAs are listed in Table V. DNA-Lipofectamine 2000 complexes (500 μl) were added to each well containing cells and medium. This was mixed gently by rocking the plate back and forth. The cells were incubated at 37˚C in a CO_2 incubator for 24-72 h until they were ready to assay for transgene expression. It was not necessary to remove the complexes or change the medium; however, the growth medium was replaced after 4-6 h without loss of transfection activity. After transfection for 48 h, total RNA was extracted and the relative mRNA expression levels were analyzed.

Cell counting kit-8 (CCK-8) assay. The CCK-8 assay was used to evaluate the proliferation of the HL60 AML cells. In brief, HL60 cells ($3x10^4$/well) were cultured in a 96-well plate with

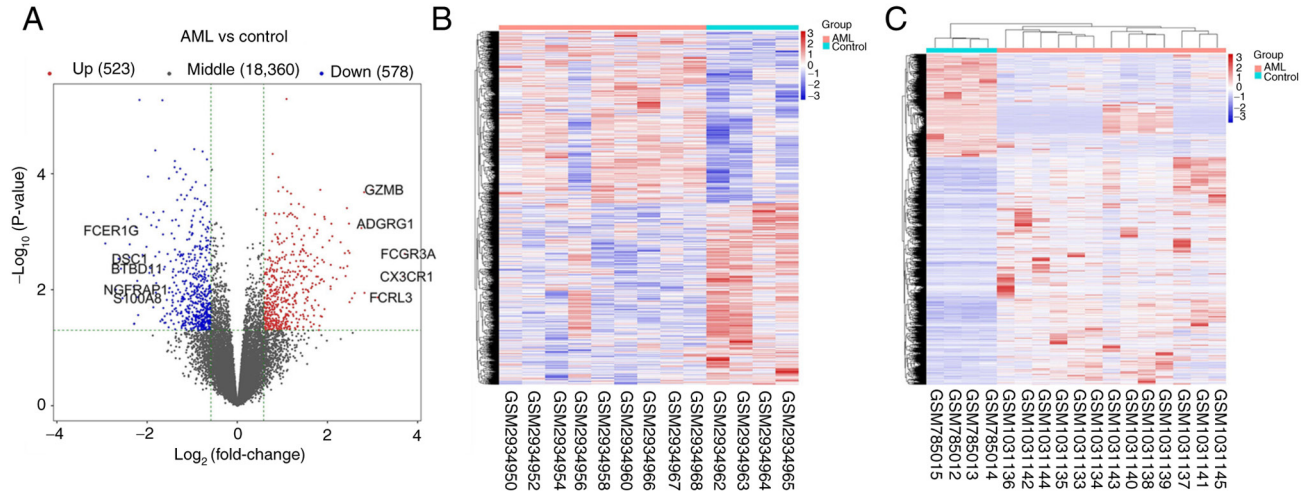

Figure 1. Comparisons of DEGs in GSE109179, GSE142699, GSE49665 and GSE14772 and DMGs in GSE42042 between AML and control samples. (A) Volcano plot of the DEGs. The right and left dotted vertical lines indicate $\log_2$FC>1 and $\log_2$FC<-1, respectively. The horizontal dotted line indicates-$\log_{10}$ P=0.05. The top five ($\log_2$FC<-1) genes are FCER1G, DSC1, BTBD11, NGFRAP1 and S100A8. The top five ($\log_2$FC>1) genes are FCGR3A, CX3CR1, FCRL3, ADGRG1 and GZMB. (B) Heatmap of the 1,101 DEGs between AML and normal samples. Red and blue indicate higher and lower expression, respectively. (C) Heatmap of the DMGs between AML and normal samples. Red and blue indicate hypermethylation and hypomethylation, respectively. DEGs, differentially expressed genes; DMGs, differentially methylated genes; AML, acute myeloid leukemia.

triplicate wells for each group. The cells were then transfected with LV003-ITGAM, LV003-TCF7, LV003-CAMK4, LV-003, si-ITGAM-1123, si-TCF7-152, si-CAMK4-365 and siRNA-NC sequences using EndoFectin™-Max (EF004; GeneCopoeia, Inc.) according to the manufacturer's protocol. Following transfection for 24 h, 100 μl culture solution containing 10 μl CCK-8 reagent (Beyotime Institute of Biotechnology) was added to each well in the absence of light and sustained in a humidity incubator at 37˚C for 24, 48 and 72 h. Subsequently, a microplate reader was used to acquire the optical density of each well at 450 nm.

Detection of cell apoptosis. The detection of HL60 AML cell apoptosis was detected using flow cytometry (Cytoflex; Beckman Coulter, Inc.). Transfected HL60 cells ($1x10^6$) were resuspended in 100 μl binding buffer, followed by the addition of 5 μl fluorochrome-conjugated Annexin V (KGA1022) and 7 μl 7-aminoactinomycin D staining solution (cat. no. 00-6993-50; eBioscience; Thermo Fisher Scientific, Inc.). A fluorescence-activated cell sorting flow cytometer (FACSAria; Becton, Dickenson and Company) and FlowJo 10.7 software (FlowJo LLC) were used to evaluate the cells and calculate the percentage of apoptotic cells.

Statistical analysis. SPSS software version 20.0 (IBM Corp.) was used to perform the analyses. Volcano plot analysis was used to evaluate DEGs as mean (AML)-mean (normal). Independent t-tests were used to calculate P-values to determine if the differences between the AML and control groups were significant for the 15 DEGs. σ2-values were determined using the unpaired t-tests. Differentially methylated regions were identified based on comparison of the methylation levels of cytosines between samples from the two groups using the Mann-Whitney U-test. Associations between characteristics and overall survival were evaluated by Cox proportional hazard models, while HR and 95% confidence interval values were described as per 1% DEG. Kaplan-Meier survival curves were drawn and compared among subgroups using log-rank tests.

Results

Identification of DEGs and DMGs in AML. Expression profile data were obtained from the GSE109179, GSE142699, GSE49665 and GSE14772 datasets, involving 87 AML samples and 40 normal samples. Following data processing, quality evaluation and analysis in R, a total of 1,101 DEGs (P<0.05 and |log FC|>1.5) were obtained, comprising 578 downregulated genes and 523 upregulated genes. The DEGs are presented in a volcano plot and a hierarchically cluster heatmap, respectively in Fig. 1A and B. Additionally, using the GSE42042 dataset, differentially methylated probe data were used to compare the AML and normal samples, as shown in the heatmap in Fig. 1C. A total of 1,187 hypomethylated and 1,551 hypermethylated genes were identified.

Identification of abnormally methylated DEGs. To identify the abnormally methylated DEGs (24), the upregulated genes that were also hypomethylated were identified, along with the downregulated genes that were also hypermethylated. In total, 45 upregulated hypomethylated genes (Fig. 2A) and 60 downregulated hypermethylated genes (Fig. 2B) were identified. The ON Gene and TS Gene databases were used to further research the abnormally methylated DEGs. The present study aimed to identify the upregulated hypomethylated genes that were oncogenes, but none were found. However, five downregulated hypermethylated TSGs [PLEKHO1, insulin like growth factor binding protein 4 (IGFBP4), BNIP3L, SUFU and MYB binding protein 1a (MYBBP1A); Fig. 3] were identified. The possibility that the abnormal hypermethylation of these TSGs led to their downregulation in AML and, consequently, to increased tumorigenesis requires investigation.

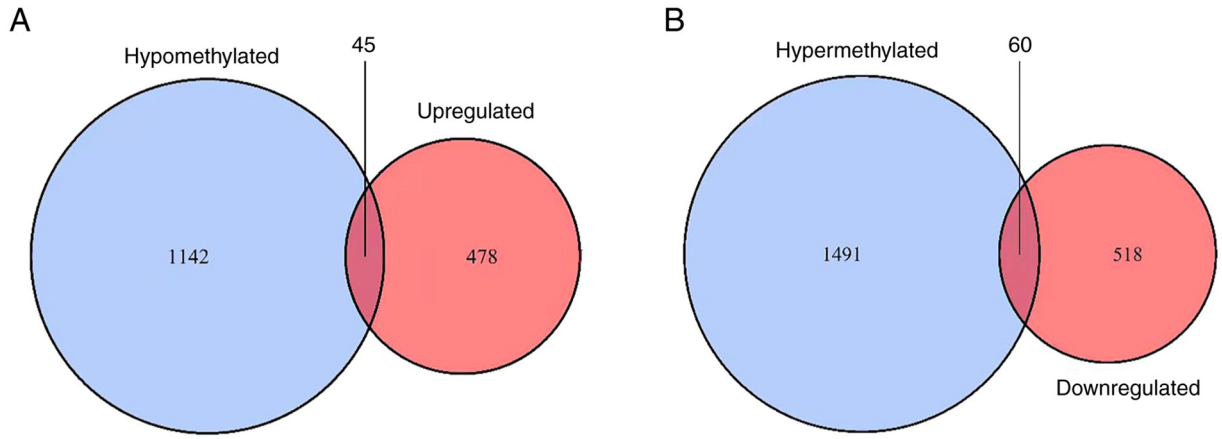

Figure 2. Identification of abnormally methylated differentially expressed genes. (A) 45 hypomethylated and upregulated genes and (B) 60 hypermethylated and downregulated genes were identified with P<0.05.

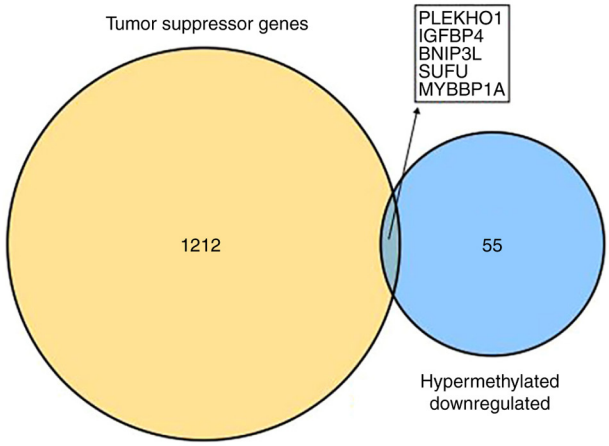

Figure 3. Identification of hypermethylated differentially expressed genes that are TSGs. Five of the 60 hypermethylated and downregulated genes were TSGs with P<0.05. TSGs, tumor suppressor genes.

Functional enrichment analyses. To search and visualize the GO BP terms and KEGG pathways associated with the upregulated hypomethylated genes and downregulated hypermethylated genes, the two lists of genes were uploaded to DAVID and the FunRich tool. The GO BP enrichment analysis, conducted using DAVID software (Fig. 4A and B) indicated that the 45 upregulated hypomethylated genes were significantly enriched in 'defense response to other organism', 'innate immune response', 'positive regulation of integrin-mediated signaling pathway', 'response to other organism', 'response to external biotic stimulus', 'cellular response to organic substance', 'platelet aggregation', 'cell surface receptor signaling pathway', 'platelet degranulation' and 'regulation of substrate adhesion-dependent cell spreading'. The 60 downregulated hypermethylated genes were significantly enriched in 'positive regulation of macro-autophagy', 'regulation of macroautophagy', 'regulation of anoikis', 'regulation of TOR signaling', 'maintenance of protein location', 'negative regulation of macroautophagy', 'cellular zinc ion homeostasis', 'positive regulation of autophagy' and 'positive regulation of TOR signaling'. Regarding the KEGG pathways (Fig. 4C and D), the 45 upregulated hypomethylated genes were significantly enriched in 'fatty acid metabolism', 'biosynthesis of unsaturated fatty acids', 'fructose and mannose metabolism', 'acute myeloid leukemia', 'PPAR signaling pathway', 'leishmaniasis', 'regulation of actin cytoskeleton', '*Staphylococcus aureus* infection', 'hematopoietic cell lineage' and 'amoebiasis'. The 60 downregulated hypermethylated genes were significantly enriched in 'longevity regulating pathway', 'Epstein-Barr virus infection', 'ferroptosis', 'signaling pathways regulating the pluripotency of stem cells', 'endometrial cancer', 'basal cell carcinoma', 'acute myeloid leukemia', 'glioma', 'B-cell receptor signaling pathway' and 'complement and coagulation cascades'. The genes associated with the pathways in Fig. 4 are presented in Table VI.

The significantly enriched pathways in the KEGG analysis were visualized using the pathview package (https://pathview.uncc.edu/). The AML signaling pathways include the MAPK, Jak-STAT, PI3K-Akt and mTOR pathways, as shown in Fig. 5. Notably, TCF7, ITGAM and PIK3CA participate in the 'acute myeloid leukemia' signaling pathway (Table VI).

PPI network construction. The online STRING database was utilized to construct PPI networks. For the 45 upregulated hypomethylated genes, the PPI network involved 45 nodes and 31 edges and showed significant PPI enrichment ($P=4.02x10^{-8}$; Fig. 6A). For the 60 downregulated hypermethylated genes, the PPI network involved 13 nodes and 8 edges, but the PPI enrichment was not found to be significant (P=79.3; Fig. 6B). The PPI network of the combination of 45 upregulated hypomethylated genes and 60 downregulated hypermethylated genes is shown, with significant PPI enrichment ($P=6.28x10^{-4}$; Fig. 6C). Finally, the PPI network of all five downregulated hypermethylated TSGs (PLEKHO1, IGFBP4, BNIP3L, SUFU and MYBBP1A) was constructed, along with their associated genes, to assess their biological functions in the network (Fig. 6D).

Validation of the selected DEGs. The data obtained by integrated bioinformatics analysis were validated using blood samples collected from patients. RT-qPCR was used to assess the levels of the 15 DEGs (TCF7, CHMP7, PIK3CA, SLC39A8, CYBB, ID3, CAMK4, SUFU, PLEKHO1, BNIP3L, VCL, ZBP1, TFDP1, ITGAM and ADRB2), 10 of which were downregulated

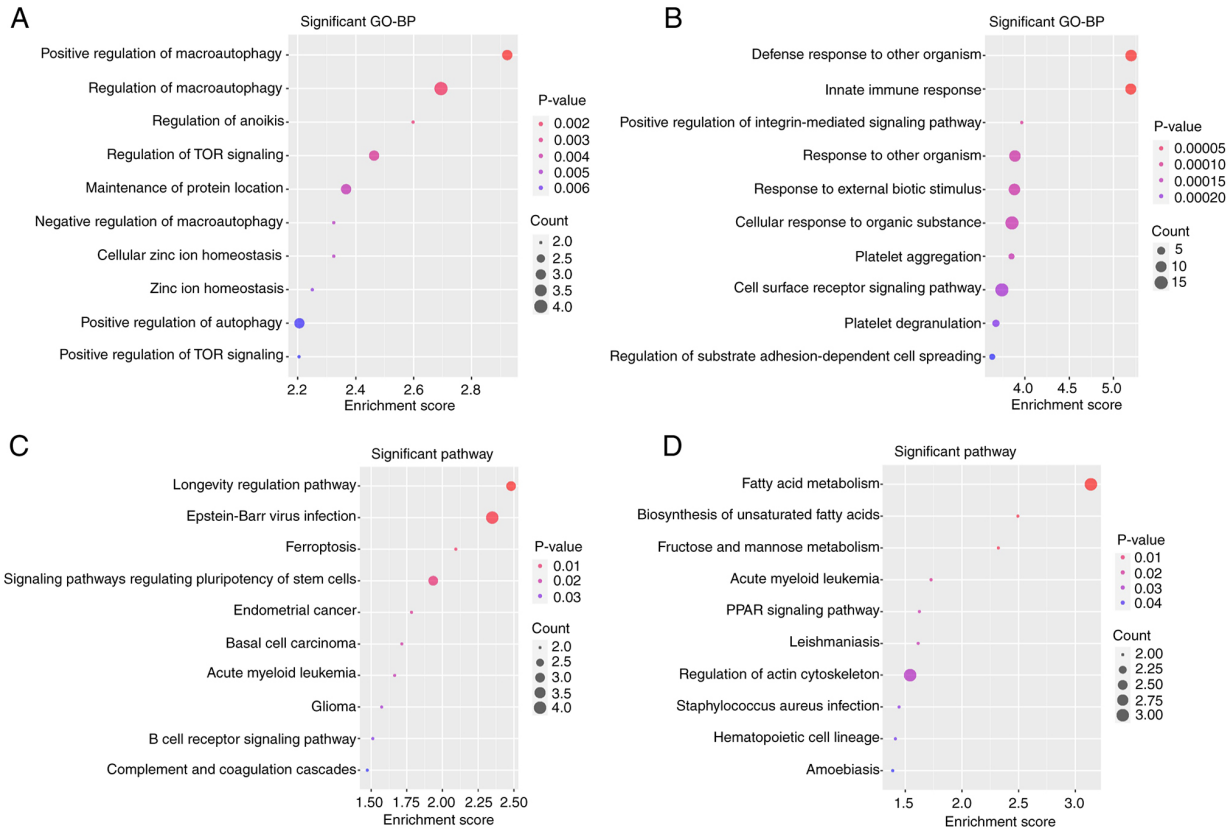

Figure 4. Bubble diagrams of enrichment results for aberrantly methylated differentially expressed genes. Deeper red indicates higher enrichment P-values. Significantly enriched GO BP terms for the (A) 45 upregulated hypomethylated genes and (B) 60 downregulated hypermethylated genes ranked by P-value using Database for Annotation, Visualization and Integrated Discovery software. Top ten KEGG pathways involving the (C) 45 upregulated hypomethylated genes and (D) 60 downregulated hypermethylated genes ranked by P-value using FunRich software. GO, Gene Ontology; BP, biological process; KEGG, Kyoto Encyclopedia of Genes and Genomes.

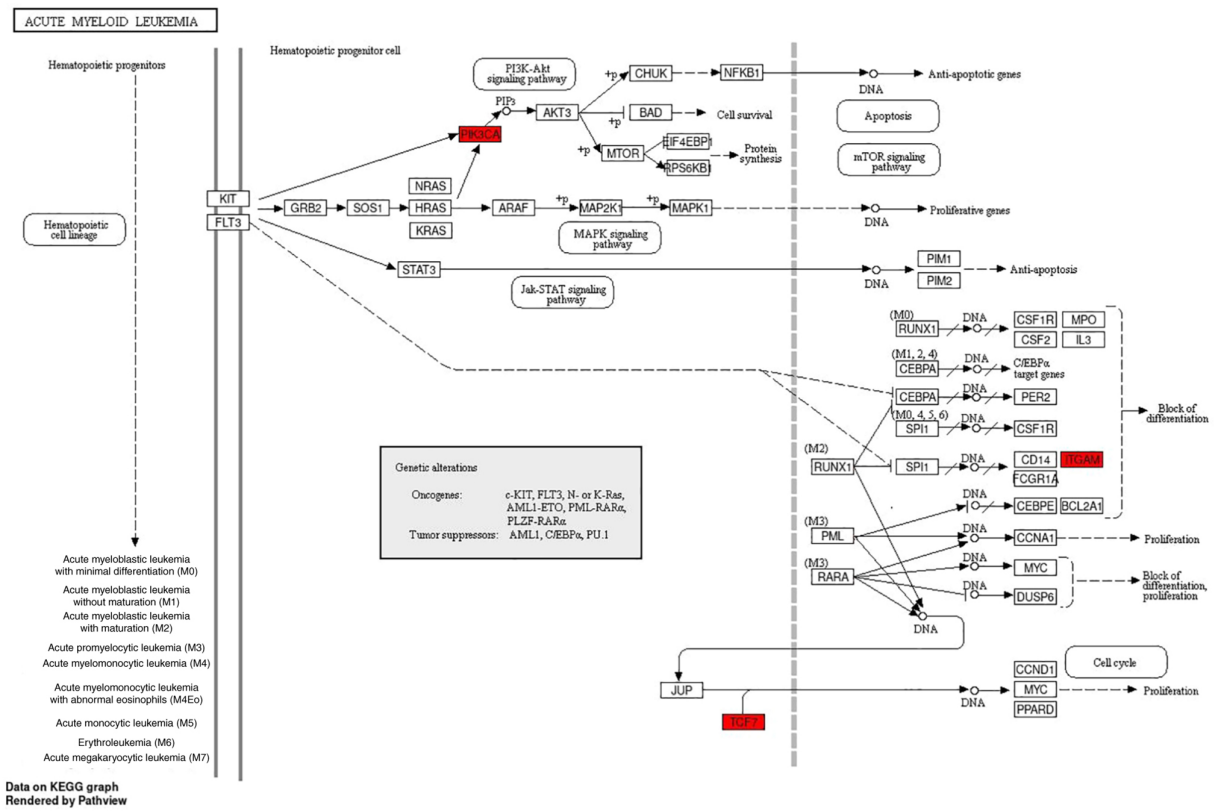

Figure 5. Signaling pathways in acute myeloid leukemia.

Table VI. Pathways and their associated genes.

Pathway	Genes
Acute myeloid leukemia	ITGAM, PIK3CA, TCF7
B cell receptor signaling pathway	CR2, LYN, PIK3CA
Longevity regulating pathway	CAMK4, PIK3CA, SESN3
Fructose and mannose metabolism	GMDS, SORD
Regulation of actin cytoskeleton	DIAPH2, ITGAM, PIK3CA, VCL
Ferroptosis	CYBB, SLC39A8
Signaling pathways regulating pluripotency of stem cells	ID3, PIK3CA, TCF7
Fatty acid metabolism	CPT1A, FADS1
Endometrial cancer	PIK3CA, TCF7
Basal cell carcinoma	SUFU, TCF7
Necroptosis	CHMP7, CYBB, ZBP1
Glioma	CAMK4, PIK3CA
Leishmaniasis	CYBB, ITGAM
Epstein-Barr virus infection	CR2, LYN, PIK3CA
TGF-beta signaling pathway	ID3, TFDP1
cAMP signaling pathway	ADRB2, CAMK4, PIK3CA
Hematopoietic cell lineage	CR2, ITGAM
Defense response to other organism	BNIP3L, C1R, CD244, CR2, CYBB, FLNA, GBP1, ITGAM, KLRG1, LYN, SIGLEC10, ZBP1
Positive regulation of macroautophagy	ADRB2, BNIP3L, SESN3, SMCR8
Defense response	BNIP3L, C1R, CAMK4, CD244, CR2, CYBB, FLNA, GBP1, IGFBP4, ITGAM, KLRG1, LYN, SIGLEC10, ZBP1
Innate immune response	C1R, CD244, CR2, CYBB, GBP1, ITGAM, KLRG1, LYN, SIGLEC10, ZBP1
Positive regulation of autophagosome maturation	ADRB2, SMCR8
Positive regulation of integrin-mediated signaling pathway	FLNA, LIMS1
Regulation of macroautophagy	ADRB2, BNIP3L, PIK3CA, SESN3, SMCR8
Anoikis	PIK3CA, TFDP1
Positive regulation of autophagy	ADRB2, BNIP3L, SESN3, SMCR8
Regulation of substrate adhesion-dependent cell spreading	FLNA, GBP1, LIMS1
Response to other organism	BNIP3L, C1R, CD244, CR2, CYBB, FLNA, GBP1, ITGAM, KLRG1, LYN, SIGLEC10, ZBP1
Response to external biotic stimulus	BNIP3L, C1R, CD244, CR2, CYBB, FLNA, GBP1, ITGAM, KLRG1, LYN, SIGLEC10, ZBP1
Cellular response to organic substance	ADRB2, CPT1A, CYBB, EHD1, FLNA, GBP1, ID3, ITGAM, LIMS1, LYN, MAP4K1, OSM, PIK3CA, PTPN12, SESN3, TCF7, TGFBR3
Regulation of TOR signaling	PIK3CA, SESN3, SMCR8
Cell surface receptor signaling pathway	ADRB2, CR2, CYBB, FLNA, GBP1, GMDS, ITGAM, KLRG1, LIMS1, LYN, OSM, PIK3CA, PTPN12, SUFU, TCF7, TGFBR3
Negative regulation of macroautophagy	PIK3CA, SMCR8
Positive regulation of TOR signaling	PIK3CA, SMCR8
Platelet degranulation	FLNA, LYN, VCL
Platelet aggregation	FLNA, VCL

and hypermethylated and 5 of which were upregulated and hypomethylated according to the bioinformatics analysis. The results of the RT-qPCR analysis indicated that the expression levels of 6 genes, namely CAMK4, CYBB, SLC39A8, SUFU and TCF7, matched the bioinformatics data, being significantly lower ($P<0.05$) in the AML samples compared with the control samples. Strong associations between the RT-qPCR results and the bioinformatics data were observed. Nevertheless, the

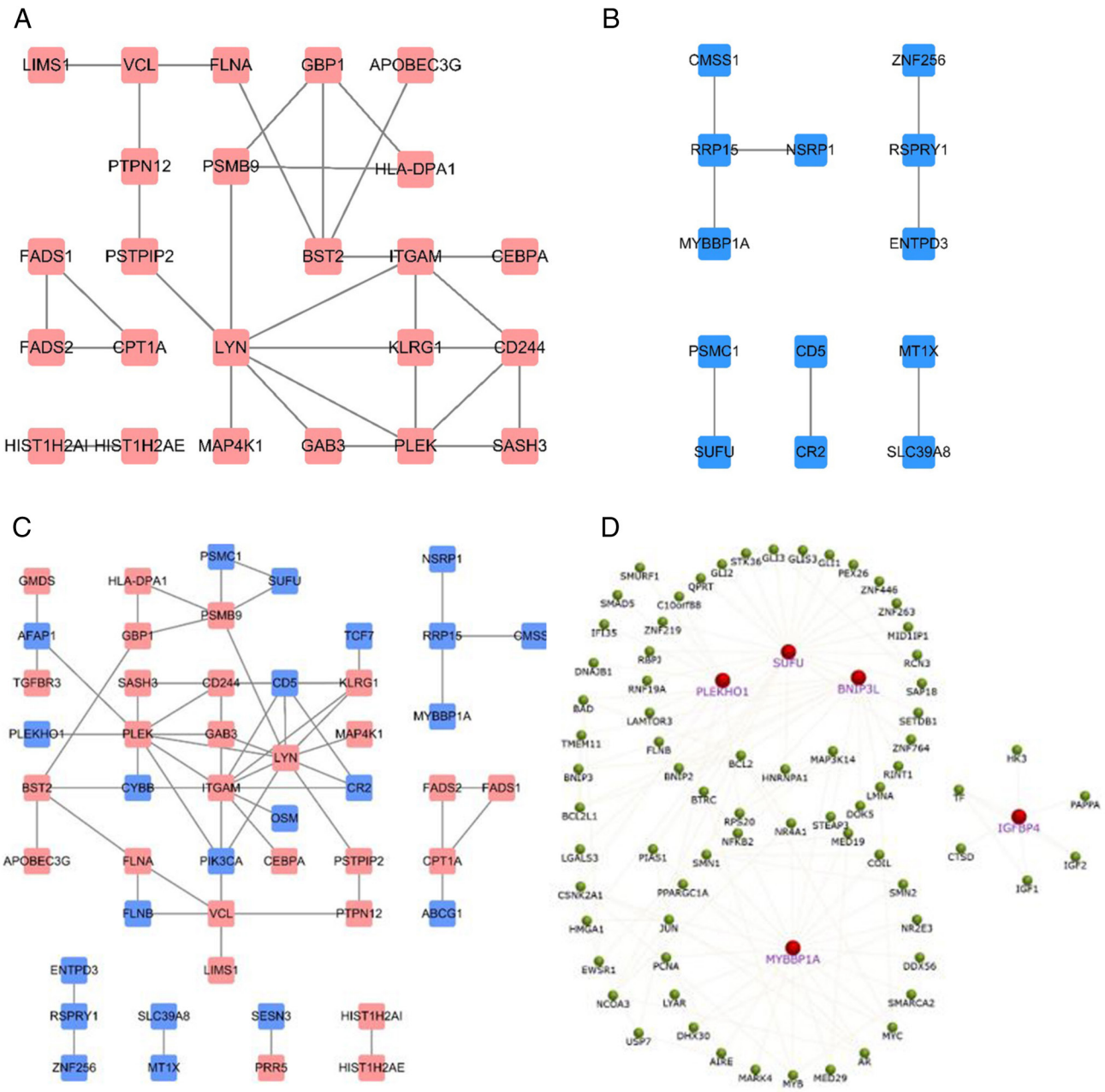

Figure 6. PPI networks of the abnormally methylated differentially expressed genes. PPI networks of (A) the main connections of 45 upregulated hypomethylated genes, (B) 60 downregulated hypermethylated genes and (C) all 105 genes, constructed using the STRING database and FunRich software. (D) PPI network of the five downregulated hypermethylated tumor suppressor genes and their associated genes, created using FunRich software. PPI, protein-protein interaction.

expression levels of ITGAM and VCL did not correspond with those in the bioinformatics analyses; ITGAM and VCL were upregulated in AML in the bioinformatics analysis but significantly downregulated ($P<0.05$) in the AML samples compared with the control samples. The remaining eight genes (PIK3CA, BNIP3L, PLEKHO1, ADRB2, CHMP7, ID3, TFDP1 and ZBP1) did not exhibit statistically significant differences between the patients with AML and the controls (Fig. 7). Regarding the methylation status of the promoters of the six DEGs assessed using next-generation sequencing-based bisulfite sequencing/PCR (Table SI), the methylation status of CAMK4 promoters was higher in patients with AML compared with the healthy controls ($P<0.05$), which was consistent with the bioinformatics analysis, while the four genes CYBB, SLC39A8, SUFU and VCL did not exhibit statistically significant differences between the patients with AML and the healthy controls (Fig. 8). It was also observed that the methylation status of ITGAM promoters in the samples did not correspond with that in the bioinformatics analyses; the bioinformatics analysis indicated that ITGAM was hypomethylated, whereas the TBS data showed that ITGAM was significantly hypermethylated in patients with AML compared with the healthy controls ($P<0.05$).

Survival analysis. To assess the associations between the AML survival rates and DEGs, a survival analysis using TCGA data was performed. Kaplan-Meier survival curves

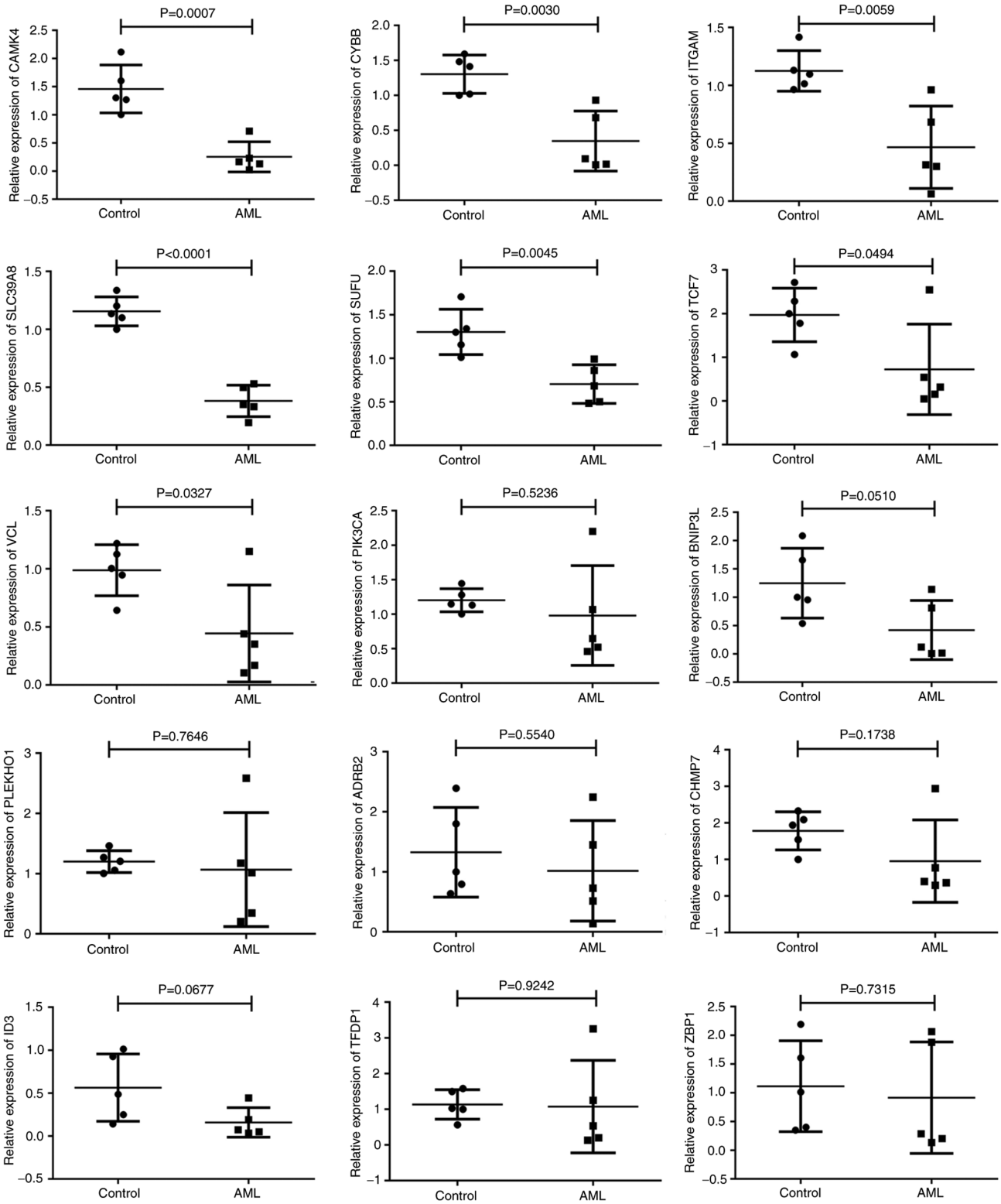

Figure 7. Validation of gene expression results in clinical samples. Scatter diagrams of the expression of 15 genes in normal and AML samples using reverse transcription-quantitative PCR. AML, acute myeloid leukemia. CAMK4, calcium/calmodulin dependent protein kinase IV; CYBB, cytochrome B-245 β chain; ITGAM, integrin α M; SCL39A8, solute carrier family 39 member 8; SUFU, SUFU negative regulator of Hedgehog signaling; TCF7, transcription factor 7; VCL, vinculin; PIK3CA, phosphatidylinositol-4,5-bisphosphonate 3-kinase catalytic subunit α; BNIP3L, BCL2 interacting protein 3 like; PLEKHO1, pleckstrin homology domain containing O1; ADRB2, adrenoceptor β 2; CHMP7, charged multivesicular body protein 7; ID3, inhibitor of DNA binding 3, HLH protein; TFDP1, transcription factor Dp-1; ZBP1, Z-DNA binding protein 1, transcription factor Dp-ZBP1.

were constructed for high and low expression subgroups for six downregulated hypermethylated genes (TCF7, SLC39A8, CYBB, SUFU, BNIP3L and CAMK4) and two upregulated hypomethylated genes (VCL and ITGAM). The gene expression subgroups were compared using log-rank tests. The results revealed that upregulated ITGAM, BNIP3L, CYBB and VCL,

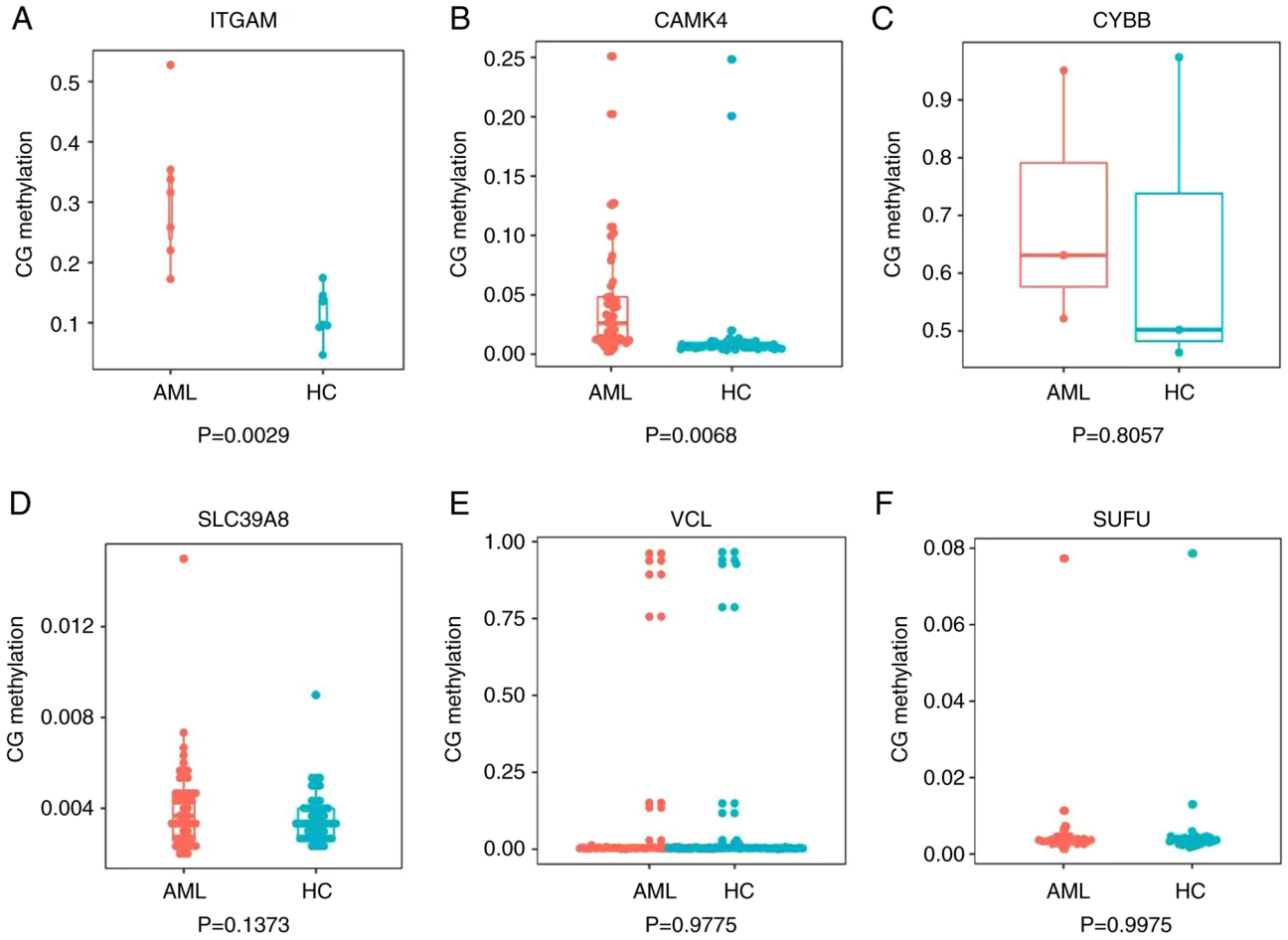

Figure 8. Validation of gene methylation results. Box plots showing the methylation status in the promoters of six genes obtained using next-generation sequencing-based bisulfite sequencing/PCR. (A) ITGAM, (B) CAMK4, (C) CYBB, (D) SCL39A8, (E) VCL and (F)SUFU. ITGAM, integrin α M; CAMK4, calcium/calmodulin dependent protein kinase IV; CYBB, cytochrome B-245 β chain; SCL39A8, solute carrier family 39 member 8; VCL, vinculin; SUFU, SUFU negative regulator of Hedgehog signaling.

as well as downregulated CAMK4 and TCF7, were associated with a low probability of survival in patients with AML; however, downregulated ITGAM, BNIP3L, CYBB and VCL, as well as upregulated CAMK4 and TCF7, were associated with a high probability of survival in patients with AML. At the same time, it was found that upregulated SLC39A8, as well as downregulated SUFU, were associated with a high probability of survival in patients with AML, and downregulated SLC39A8, as well as upregulated SUFU, were associated with a low probability of survival in patients with AML (Fig. 9).

TCF7 and ITGAM overexpression inhibits while CAMK4 and TCF7 downregulation increases cell proliferation without affecting cell apoptosis. To further investigate the effects of certain genes, ITGAM, TCF7 and CAMK4 were overexpressed or knocked down in HL60 cells (Figs. S1 and S2). Subsequently, HL60 cell proliferation was analyzed, and the results revealed that the overexpression of TCF7 and ITGAM significantly suppressed cell proliferation (Fig. 10A and B). However, the overexpression of CAMK4 did not have a significant effect on HL60 cell proliferation (Fig. 10C). The downregulation of CAMK4 and TCF7 significantly increased cell proliferation (Fig. 10D and E), but the downregulation of ITGAM had no significant effect on cell proliferation (Fig. 10F). The apoptotic percentages of the HL60 cells were also measured. Flow cytometric results indicated that neither the overexpression nor the downregulation of TCF7, ITGAM and CAMK4 induced cell apoptosis (Fig. 11).

Discussion

In the present study, the NCBI GEO database was used to obtain gene expression and methylation profiles on patients with AMI. In total, four gene expression profile datasets, namely GSE109179, GSE142699, GSE49665 and GSE14772, and one gene methylation profile dataset, namely GSE42042, were acquired from the NCBI GEO database. R software is an important tool for analyzing microarray data, as it can be used to compare different groups of samples and identify genes that are differentially expressed under various conditions. Additionally, bioinformatics analyses of the mechanisms underlying AML occurrence and development may provide findings useful in the diagnosis, treatment and prognostic evaluation of patients with AML. Using bioinformatics analyses, the present study identified no hypomethylated oncogenes and five downregulated hypermethylated TSGs in AML. Functional enrichment of differentially expressed

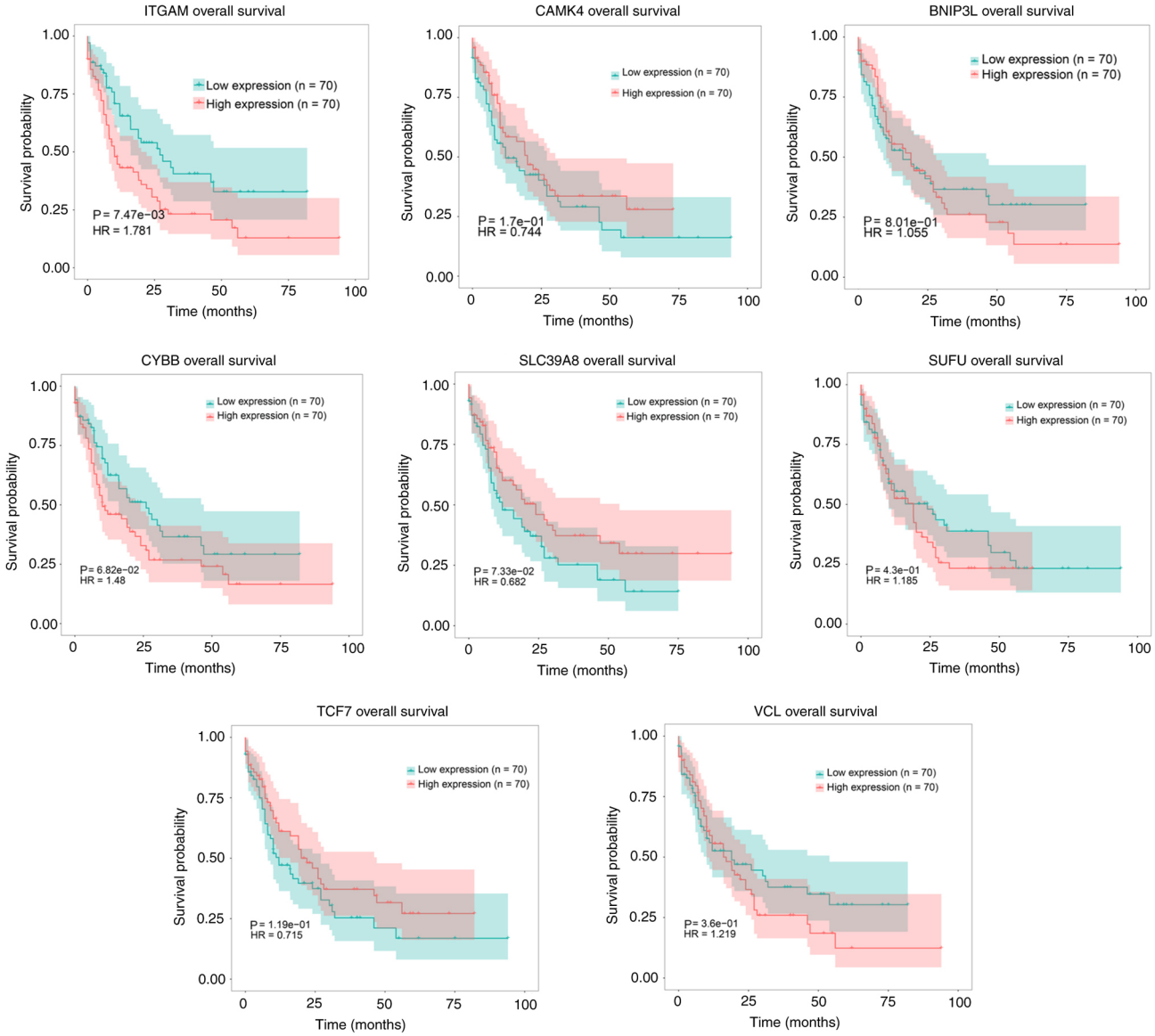

Figure 9. Associations of differentially expressed gene expression with overall survival of patients with acute myeloid leukemia in The Cancer Genome Atlas database. Kaplan-Meier survival curves for high and low expression subgroups according to the median value of each gene. P-values were determined using the log-rank test. ITGAM, integrin α M; CAMK4, calcium/calmodulin dependent protein kinase IV; BINP3L, BCL2 interacting protein 3 like; CYBB, cytochrome B-245 β chain; SLC39A8, solute carrier family 39 member 8; SUFU, SUFU negative regulator of Hedgehog signaling; TCF7, transcription factor 7; VCL, vinculin.

and methylated genes revealed that abnormal methylation influences certain pathways and their hub genes. These data provide novel perspectives on the pathogenic mechanisms of AML.

The enriched GO terms associated with the abnormally methylated DEGs were found to be associated with control of the immune response. The present study indicated that the upregulated hypomethylated genes were significantly enriched in the 'positive regulation of macroautophagy' and the 'regulation of mTOR signaling' GO BPs. The mTOR signaling pathway participates in cell apoptosis and autophagy (25), which may influence the prognosis and progression of AML. The downregulated hypermethylated genes were significantly enriched in the 'defense response to other organism' and 'innate immune response' GO BPs. KEGG pathway analysis revealed that the upregulated hypomethylated genes were significantly enriched in the 'longevity regulating pathway'. The enriched KEGG pathways were also found to be associated with immunoregulation. These findings may be relevant to the chemotherapy and other treatment measures used for patients with AML.

Pathway mapping of the KEGG data demonstrated the enrichment of aberrantly methylated DEGs in the regulation of AML signaling pathways, including the MAPK, Jak-STAT, PI3K-Akt and mTOR pathways. TCF7, ITGAM and PIK3CA participate in the 'acute myeloid leukemia' signaling pathway, which has been recognized as a key pathway in cancer (20). The PI3K/AKT/mTOR pathway is considered crucial pathway in malignant tumors as it is commonly beneficial to survival via the activation of anti-apoptotic factors and the suppression of pro-apoptotic factors; it plays a key role in tumor stem-cell self-renewal and

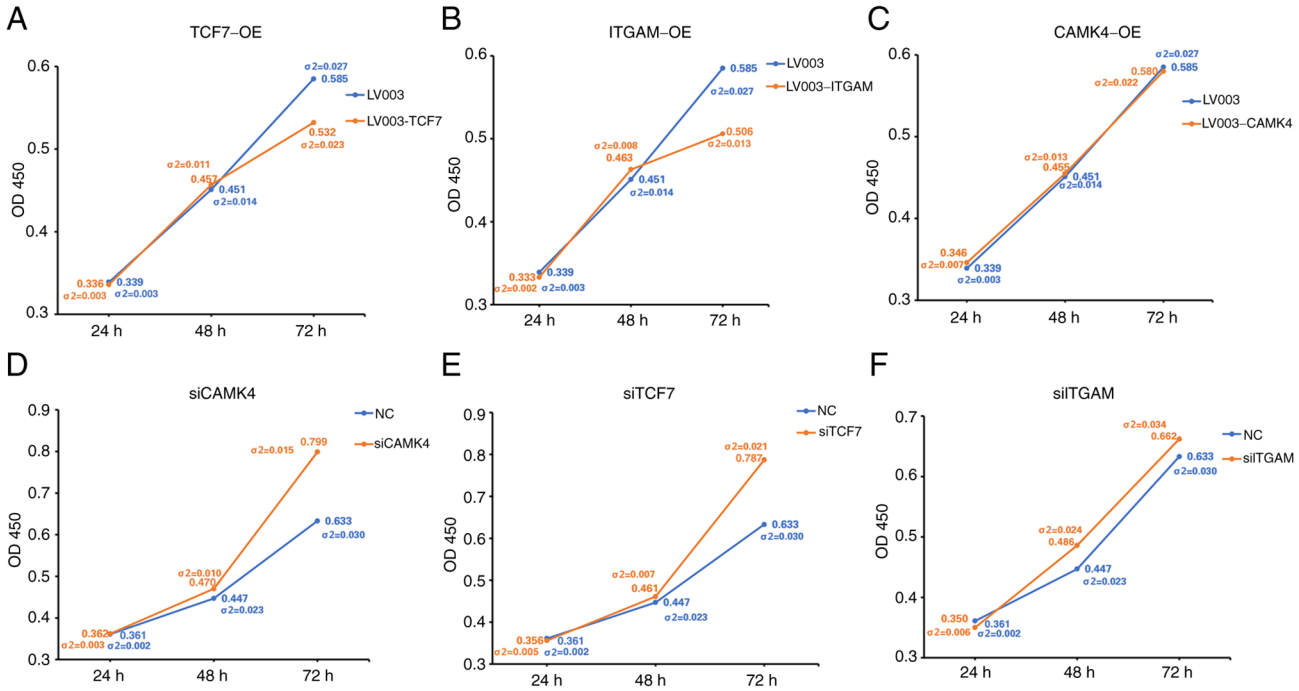

Figure 10. Viability of HL60 cells with gene overexpression or knockdown. Viability of HL60 cells with overexpression of (A) TCF7, (B) ITGAM and (C) CAMK4 or knockdown of (D) CAMK4, (E) TCF7 and (F) ITGAM. (A), (B), (D) and (E) σ2<0.05. σ2-values were determined using the unpaired t-tests. Each time point for each group has two values. One value is the mean OD measurement, and the other (σ2) the standard deviation. TCF7, transcription factor 7; ITGAM, integrin α M; CAMK4, calcium/calmodulin dependent protein kinase IV; OE, overexpression; OD450, optical density at 450 nm.

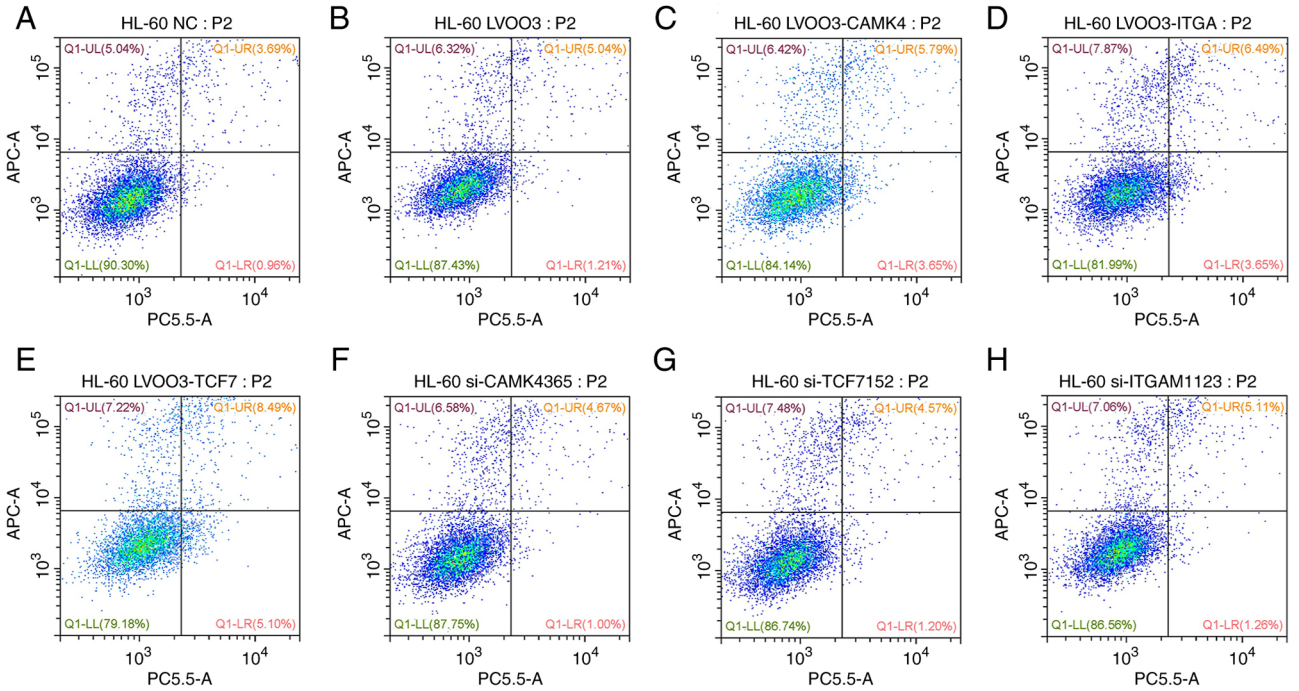

Figure 11. Apoptosis of HL60 cells with gene expression or knockdown. Flow cytometry plots for cells transfected with (A) NC, (B) LV003 empty vector control, (C) CAMK4 overexpression vector, (D) ITGAM overexpression vector, (E) TCF7 overexpression vector, (F) si-CAMK4, (G) si-TCF7 and (H) si-ITGAM. NC, negative control siRNA; si, small interfering; CAMK4, calcium/calmodulin dependent protein kinase IV; ITGAM, integrin α M; TCF7, transcription factor 7.

the resistance to radiotherapy or chemotherapy (21), which are considered to be the fundamental reason for ineffective treatment and neoplasm recurrence. The present data suggest the importance of these pathways in AML; however, further research is required to validate these data. The Jak-STAT pathway is a common pathway associated with cytokine transduction, which is widely involved in cell proliferation, differentiation, apoptosis and inflammation (26). Further studies are essential to validate the importance of the role of this pathway in AML.

PPI networks were established based on the 105 abnormally methylated DEGs. The PPI network of the 45 upregulated hypomethylated genes revealed that ITGAM was the most highly interconnected node, and ITGAM was identified to be most enriched in the 'acute myeloid leukemia' pathways. The PPI network of the 60 downregulated hypermethylated genes revealed that ribosomal RNA processing 15 homolog (RRP15) was the most interconnected node, with only three connected nodes. When all 105 genes were combined into a PPI network, ITGAM and LYN were the top interconnected nodes. The PPI network of the five downregulated hypermethylated TSGs indicated that SUFU was the top interconnected node, and SUFU was identified as mainly enriched in the 'basal cell carcinoma' pathway. TCF7, which was found to be the most connected gene in this study (22), maps on the TCF element in the AML pathway and participates in cell proliferation. ITGAM represents the most connected node in the PPI network. ITGAM is regarded as a flag for myeloid-derived suppressor cells that can mediate tumor immune escape and treatment failure. It has been evaluated in patients with AML, and a close association between ITGAM overexpression and an unfavorable AML prognosis was identified (5). Overall, the findings are consistent with those of the present study, which demonstrated an association between high ITGAM expression and an unfavorable AML prognosis in the survival analysis. This result requires confirmation in further experiments. The integrated bioinformatics analyses revealed that ITGAM was upregulated and hypomethylated, whereas the validation results showed that ITGAM was downregulated and hypermethylated. Further research is required to clarify these results. It has been reported that the upregulation of PIK3CA may downregulate its target gene, PIK3R2, which affects the PTEN/PIK3CA/AKT pathway and decreases the proliferation, transplantation and aggression of tumor cells (27). A previous study demonstrated that signaling pathways in AML serve an essential role in resistance to radiotherapy and chemotherapy and the self-renewal capacity of tumor stem cells (28). The significance of the roles of the aforementioned genes in AML may be interpreted on the basis of known data. However, further research on these genes is warranted to fully determine their roles in AML.

Seven major downregulated hypermethylated genes identified in the bioinformatics analysis in the present study were TCF7, CHMP7, PIK3CA, SLC39A8, CYBB, ID3 and CAMK4. These genes are enriched in metabolic pathways that are associated with AML and play a key role in PPI networks. CHMP7 has been found to be unusually downregulated in spinal and bulbar muscular atrophy, while SLC39A8 mutations can result in severe type II glycosylation disease (29). Previous data indicate that CYBB induces reactive oxygen species; the researchers discovered an association between lower CYBB expression and improved survival in AML (30). ID3 is a member of the ID family that influences cell proliferation and differentiation (31). However, it is primarily expressed in lymphoblastic leukemias rather than AML (32). Lastly, CAMK4 is a novel drug target for the treatment of autoimmune/inflammatory diseases that has been shown to be downregulated in hepatocellular carcinoma tissues (33).

The five major upregulated hypomethylated genes identified using bioinformatics were VCL, ZBP1, TFDP1, ITGAM and ADRB2; they are enriched in star pathways that are associated with AML and have great connectivity to play a key role in PPI networks. These genes have seldom been reported.

VCL is a cytoskeletal protein that is involved in cell-cell and cell-matrix interactions (34), and may be involved in securing F-actin to the membrane. ZBP1 is an immune sensor of nucleic acids. The activation of this protein leads to inflammation, necroptosis, apoptosis and pyroptosis (35). TFDP1 has been shown to be a latent target gene of miR-4711-5, which contributes to cell cycle progression from the G_1 to the S phase (36). Three major downregulated hypermethylated TSGs were SUFU, PLEKHO1 and BNIP3L. SUFU is a negative regulator of the Hedgehog signaling pathway, which has been implicated in cancer progression in several organs (37); it has been shown to inhibit cancer progression by suppressing the activation of Hedgehog signaling in cancer cells, thereby inducing apoptosis. PLEKHO1 is involved in macrophage proliferation and migration and can interact with Akt via its leucine zipper motif and thereby suppress PI3K/Akt signalling (38). AML cells lacking BNIP3L have been reported to display a high sensitivity to mitochondria-targeting drugs (39), suggesting that BNIP3L may be a novel drug target for AML.

In vitro experiments were performed in the present study to verify the results in the samples from patients with AML. The results revealed that the overexpression of TCF7 and ITGAM inhibited cell proliferation, the downregulation of CAMK4 and TCF7 enhanced cell proliferation, but the overexpression or downregulation of TCF7, ITGAM and CAMK4 did not induce cell apoptosis.

The present study has certain limitations. Clinical data and prognoses were not examined due to the lack of available data. Thus, further research in this area is necessary. Further mechanistic analyses are required to perform a substantial verification of the results in association with AML.

In conclusion, in the present study, integrated bioinformatics analyses were performed to identify abnormally methylated and differentially expressed oncogenes and TSGs, and their associated pathways and functions. These results provide insight into the molecular mechanisms underlying the initiation and development of AML. The 15 selected genes, comprising 10 downregulated hypermethylated genes (TCF7, CHMP7, PIK3CA, SLC39A8, CYBB, ID3, CAMK4, SUFU, PLEKHO1 and BNIP3L) and five upregulated hypomethylated genes (VCL, ZBP1, TFDP1, ITGAM and ADRB2), underwent validation using RT-qPCR. In the future, at least some of these genes may be utilized for precise AML diagnosis and therapy, as they may serve as abnormal methylation-based biomarkers and treatment targets. The present study employed several datasets rather than a single dataset to increase the validity of the findings. The lack of availability of additional data is a limitation of the present study. Therefore, additional samples and further assessments are necessary to confirm the relevance of the candidate AML genes.

Acknowledgements

Not applicable.

Funding

The present study was financially supported by the Science and Technology Program of Guangzhou (grant no. 202002030022).

Availability of data and materials

All data generated or analyzed during this study are included in this published article.

Authors' contributions

WWC conceived and designed the study, obtained the funding and provided administrative support. JQ contributed to analyzing the data. DBL analysed and interpreted the data. JQ and DBL confirm the authenticity of all the raw data. WWC, LJZ and HXX conducted the data analysis and interpretation. All authors wrote the manuscript, and all authors read and approved the final version of the manuscript.

Ethics approval and consent to participate

Ethics approval was obtained from the Ethics Committee of Guangzhou Twelfth People's Hospital (Guangzhou, China; approval no. 2020046). The patients provided written informed consent for collection of their samples and their use in scientific research.

Patient consent for publication

Not applicable.

Competing interests

The authors declare that they have no competing interests.

References

1. Alvarez MC, Maso V, Torello CO, Ferro KP and Saad STO: The polyphenol quercetin induces cell death in leukemia by targeting epigenetic regulators of pro-apoptotic genes. Clin Epigenetics 10: 139, 2018.
2. Casano K, Meddaugh H, Zambrano RM, Marble M, Torres JI and Lacassie Y: Gorlin-like phenotype in a patient with a PTCH2 variant of uncertain significance. Eur J Med Genet 63: 103842, 2020.
3. Hao BB, Li XJ, Jia XL, Wang YX, Zhai LH, Li DZ, Liu J, Zhang D, Chen YL, Xu YH, *et al*: The novel cereblon modulator CC-885 inhibits mitophagy via selective degradation of BNIP3L. Acta Pharmacol Sin 41: 1246-1254, 2020.
4. Wei Y, Xiong X, Li X, Lu W, He X, Jin X, Sun R, Lyu H, Yuan T, Sun T and Zhao M: Low-dose decitabine plus venetoclax is safe and effective as post-transplant maintenance therapy for high-risk acute myeloid leukemia and myelodysplastic syndrome. Cancer Sci 112: 3636-3644, 2021.
5. Hu L, Gao Y, Shi Z, Liu Y, Zhao J, Xiao Z, Lou J, Xu Q and Tong X: DNA methylation-based prognostic biomarkers of acute myeloid leukemia patients. Ann Transl Med 7: 737, 2019.
6. Zhang X, Feng H, Li D, Liu S, Amizuka N and Li M: Identification of differentially expressed genes induced by aberrant methylation in oral squamous cell carcinomas using integrated bioinformatic analysis. Int J Mol Sci 19: 1698, 2018.
7. Xi Y, Lin Y, Guo W, Wang X, Zhao H, Miao C, Liu W, Liu Y, Liu T, Luo Y *et al*: Multi-omic characterization of genome-wide abnormal DNA methylation reveals diagnostic and prognostic markers for esophageal squamous-cell carcinoma. Signal Transduct Target Ther 7: 53, 2022.
8. Itoh S, Yamazaki J, Iwahana M and Tsukamoto A: Olsalazine inhibits cell proliferation and DNA methylation in canine lymphoid tumor cell lines. Pol J Vet Sci 24: 515-523, 2021.
9. Shen S, Wang G, Shi Q, Zhang R, Zhao Y, Wei Y, Chen F and Christiani DC: Seven-CpG-based prognostic signature coupled with gene expression predicts survival of oral squamous cell carcinoma. Clin Epigenetics 9: 88, 2017.
10. Grencewicz DJ, Romigh T, Thacker S, Abbas A, Jaini R, Luse D and Eng C: Redefining the PTEN promoter: Identification of novel upstream transcription start regions. Hum Mol Genet 30: 2135-2148, 2021.
11. Pramodh S, Raina R, Hussain A, Bagabir SA, Haque S, Raza ST, Ajmal MR, Behl S and Bhagavatula D: Luteolin causes 5'CpG demethylation of the promoters of TSGs and modulates the aberrant histone modifications, restoring the expression of TSGs in human cancer cells. Int J Mol Sci 23: 4067, 2022.
12. Huang S, Zhang B, Fan W, Zhao Q, Yang L, Xin W and Fu D: Identification of prognostic genes in the acute myeloid leukemia microenvironment. Aging (Albany NY) 11: 10557-10580, 2019.
13. Kanehisa M and Goto S: KEGG: Kyoto encyclopedia of genes and genomes. Nucleic Acids Res 28: 27-30, 2000.
14. Chin CH, Chen SH, Wu HH, Ho CW, Ko MT and Lin CY: cytoHubba: Identifying hub objects and sub-networks from complex interactome. BMC Syst Biol 8 (Suppl 4): S11, 2014.
15. Ashburner M, Ball CA, Blake JA, Botstein D, Butler H, Cherry JM, Davis AP, Dolinski K, Dwight SS, Eppig JT, *et al*: Gene ontology: Tool for the unification of biology. The gene ontology consortium. Nat Genet 25: 25-29, 2000.
16. Shen Y, Pan X and Yang J: Gene regulation and prognostic indicators of lung squamous cell carcinoma: TCGA-derived miRNA/mRNA sequencing and DNA methylation data. J Cell Physiol 234: 22896-22910, 2019.
17. Knaus HA, Berglund S, Hackl H, Blackford AL, Zeidner JF, Montiel-Esparza R, Mukhopadhyay R, Vanura K, Blazar BR, Karp JE, *et al*: Signatures of CD8+ T cell dysfunction in AML patients and their reversibility with response to chemotherapy. JCI Insight 3: e120974, 2018.
18. Rommer A, Steinleitner K, Hackl H, Schneckenleithner C, Engelmann M, Scheideler M, Vlatkovic I, Kralovics R, Cerny-Reiterer S, Valent P, *et al*: Overexpression of primary microRNA 221/222 in acute myeloid leukemia. BMC Cancer 13: 364, 2013.
19. Tanaka M, Oikawa K, Takanashi M, Kudo M, Ohyashiki J, Ohyashiki K and Kuroda M: Down-regulation of miR-92 in human plasma is a novel marker for acute leukemia patients. PLoS One 4: e5532, 2009.
20. Pérez C, Pascual M, Martín-Subero JI, Bellosillo B, Segura V, Delabesse E, Álvarez S, Larrayoz MJ, Rifón J, Cigudosa JC, *et al*: Aberrant DNA methylation profile of chronic and transformed classic Philadelphia-negative myeloproliferative neoplasms. Haematologica 98: 1414-1420, 2013.
21. Liu F, Wei T, Liu L, Hou F, Xu C, Guo H, Zhang W, Ma M, Zhang Y, Yu Q and Wang J: Role of necroptosis and immune infiltration in human stanford type A aortic dissection: Novel insights from bioinformatics analyses. Oxid Med Cell Longev 2022: 6184802, 2022.
22. Livak KJ and Schmittgen TD: Analysis of relative gene expression data using real-time quantitative PCR and the 2(-Delta Delta C(T)) method. Methods 25: 402-408, 2001.
23. Abd ElHafeez S, D'Arrigo G, Leonardis D, Fusaro M, Tripepi G and Roumeliotis S: Methods to analyze time-to-event data: The cox regression analysis. Oxid Med Cell Longev 2021: 1302811, 2021.
24. Luo Y, Sun F, Peng X, Dong D, Ou W, Xie Y and Luo Y: Integrated bioinformatics analysis to identify abnormal methylated differentially expressed genes for predicting prognosis of human colon cancer. Int J Gen Med 14: 4745-4756, 2021.
25. Wang L, Jiang W, Wang J, Xie Y and Wang W: Puerarin inhibits FUNDC1-mediated mitochondrial autophagy and CSE-induced apoptosis of human bronchial epithelial cells by activating the PI3K/AKT/mTOR signaling pathway. Aging (Albany NY) 14: 1253-1264, 2022.
26. Alhadidi Q and Shah ZA: Cofilin Mediates LPS-induced microglial cell activation and associated neurotoxicity through activation of NF-κB and JAK-STAT pathway. Mol Neurobiol 55: 1676-1691, 2018.
27. Silverbush D, Grosskurth S, Wang D, Powell F, Gottgens B, Dry J and Fisher J: Cell-specific computational modeling of the PIM pathway in acute myeloid leukemia. Cancer Res 77: 827-838, 2017.

28. Stranahan AW, Berezniuk I, Chakraborty S, Feller F, Khalaj M and Park CY: Leukotrienes promote stem cell self-renewal and chemoresistance in acute myeloid leukemia. Leukemia 36: 1575-1584, 2022.
29. Malik B, Devine H, Patani R, La Spada AR, Hanna MG and Greensmith L: Gene expression analysis reveals early dysregulation of disease pathways and links Chmp7 to pathogenesis of spinal and bulbar muscular atrophy. Sci Rep 9: 3539, 2019.
30. Garcia-Manero G, Tambaro FP, Bekele NB, Yang H, Ravandi F, Jabbour E, Borthakur G, Kadia TM, Konopleva MY, Faderl S, *et al*: Phase II trial of vorinostat with idarubicin and cytarabine for patients with newly diagnosed acute myelogenous leukemia or myelodysplastic syndrome. J Clin Oncol 30: 2204-2210, 2012.
31. Park JS, Kim SM, Choi J, Jung KA, Hwang SH, Yang S, Kwok SK, Cho ML and Park SH: Interleukin-21-mediated suppression of the Pax3-Id3 pathway exacerbates the development of Sjögren's syndrome via follicular helper T cells. Cytokine 125: 154834, 2020.
32. May AM, Frey AV, Bogatyreva L, Benkisser-Petersen M, Hauschke D, Lübbert M, Wäsch R, Werner M, Hasskarl J and Lassmann S: ID2 and ID3 protein expression mirrors granulopoietic maturation and discriminates between acute leukemia subtypes. Histochem Cell Biol 141: 431-440, 2014.
33. Li Z, Lu J, Zeng G, Pang J, Zheng X, Feng J and Zhang J: MiR-129-5p inhibits liver cancer growth by targeting calcium calmodulin-dependent protein kinase IV (CAMK4). Cell Death Dis 10: 789, 2019.
34. Wang XT, Fang R, Ye SB, Zhang RS, Li R, Wang X, Ji RH, Lu ZF, Ma HH, Zhou XJ, *et al*: Targeted next-generation sequencing revealed distinct clinicopathologic and molecular features of VCL-ALK RCC: A unique case from an older patient without clinical evidence of sickle cell trait. Pathol Res Pract 215: 152651, 2019.
35. Kesavardhana S, Malireddi RKS, Burton AR, Porter SN, Vogel P, Pruett-Miller SM and Kanneganti TD: The Zα2 domain of ZBP1 is a molecular switch regulating influenza-induced PANoptosis and perinatal lethality during development. J Biol Chem 295: 8325-8330, 2020.
36. Morimoto Y, Mizushima T, Wu X, Okuzaki D, Yokoyama Y, Inoue A, Hata T, Hirose H, Qian Y, Wang J, *et al*: miR-4711-5p regulates cancer stemness and cell cycle progression via KLF5, MDM2 and TFDP1 in colon cancer cells. Br J Cancer 122: 1037-1049, 2020.
37. Zheng S, Li M, Miao K and Xu H: lncRNA GAS5-promoted apoptosis in triple-negative breast cancer by targeting miR-378a-5p/SUFU signaling. J Cell Biochem 121; 2225-2235, 2020.
38. Zhang P, Zhou C, Lu C, Li W, Li W, Jing B, Chen W, Zha Y, Zhang P, Bai C, *et al*: PLEKHO2 is essential for M-CSF-dependent macrophage survival. Cell Signal 37: 115-122, 2017.
39. Rodrigo R, Mendis N, Ibrahim M, Ma C, Kreinin E, Roma A, Berg S, Blay J and Spagnuolo PA: Knockdown of BNIP3L or SQSTM1 alters cellular response to mitochondria target drugs. Autophagy 15: 900-907, 2019.